Accepted Manuscript

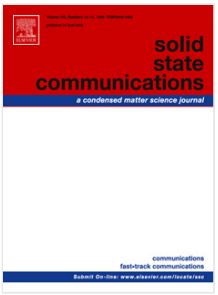

Synthesis, electrical and magnetotransport properties of polypyrrole-MWCNT nanocomposite

G. Chakraborty, K. Gupta, A.K. Meikap, R. Babu, W.J. Blau

PII: S0038-1098(11)00554-0
DOI: 10.1016/j.ssc.2011.10.018
Reference: SSC 11349

To appear in: *Solid State Communications*

Received date: 27 June 2011
Revised date: 21 September 2011
Accepted date: 16 October 2011

Please cite this article as: G. Chakraborty, K. Gupta, A.K. Meikap, R. Babu, W.J. Blau, *Solid State Communications* (2011), doi:10.1016/j.ssc.2011.10.018

Synthesis, Electrical and Magnetotransport Properties Of Polypyrrole-MWCNT Nanocomposite

G. Chakraborty[1], K.Gupta[1], A. K. Meikap[1*], R. Babu[2] and W. J. Blau[2]

[1]Department of Physics, National Institute of Technology, Durgapur
Mahatma Gandhi Avenue, Durgapur – 713 209, West Bengal, India
[2]Department of Physics, University of Dublin
Trinity College, Dublin 2, Ireland

ABSTRACT

The present work describes the preparation of nanocomposites in which the multiwall carbon nanotubes (MWCNT) have been mixed with conducting polypyrrole (PPy) via an in situ chemical oxidative preparation method. To reveal their structural, morphological and thermal properties, the composites have been characterized by x-ray diffraction, field emission scanning electron microscope, Fourier transform infrared, thermogravimetric analysis respectively. Electrical transport and magnetotransport properties have been investigated in the temperature range 77-300K in presence as well as in absence of magnetic field up to 1Tesla. The conductivities of the composites are greater than that of pure polypyrrole. All the investigated samples follow Mott's variable range hopping (VRH) theory whereas the magnetic field dependent conductivity have been explained in terms of two opposite but simultaneously acting hopping effect-wave function shrinkage and forward interference effect.

Keywords: A. Polypyrrole; A. Multi walled Carbon nanotubes; D. VRH theory; D. Charge transport

[*]***Corresponding author.*** Tel.: +91 343 2546808; fax: +91 343 2547375.

[*]***Email address:*** meikapnitd@yahoo.com (A. K. Meikap)

1. Introduction

During the last few decades, the study of conducting polymer composites has been carried out with growing interest. To enhance the application of conducting polymers, different materials of organic and inorganic origin have been used as conductive or insulating filler inside the matrix of the conducting polymer. This class of materials has a vast application in electromagnetic interference shielding, rechargeable batteries, electrodes, sensors, corrosion protection coatings, microwave absorption and so on [1-10]. Most of the conducting polymers have an extended π-conjugation system with single and double bond alteration along with polymeric backbone. They behave like semiconducting materials with low charge carrier mobility's. Their conductivities can be enhanced by several orders by inserting suitable conductive fillers inside their polymer matrix. The conductivity of the composites depend on several factors like concentration of the conductive fillers, their shape, size, orientation and the interfacial interaction between the filler and the host matrix. It depends also on the reaction temperature, time of polymerization, monomer to oxidant molar ratio and oxidizing agent. The capacity for conductive network formation depends on the geometrical shape of the filler for which the larger conductivity is found. Polypyrrole (PPy) has become one of the most important conducting polymers due to their appreciable environmental stability, higher electrical conductivity, easier synthesis, solubility in different solvents [11-12]. It has a potential application in the field of composite materials, tissue engineering, actuator, supercapacitor, electronic and optoelectronic devices [13-18]. Carbon nanotubes (CNT) also have received significant attention for their unique mechanical, electrical, thermal and magnetic properties that have been used in the field of nanocomposites materials, nanoelectronic devices and so on [19-20]. The large aspect ratio of CNTs has made them effective as conductive fillers in polymers [21]. Introduction of CNTs into the polymer matrix improve not only the stability of the polymers but also enhance the mechanical and electrical properties [22-23]. According to Guo et al [24], formation of a π-π non-covalent bond between the delocalized π electrons of the conducting polymer and the delocalized π electrons of the p-orbit of the carbon atoms of the CNTs reduce the energy of the composites to form a new stable system. Thus the conducting polypyrrole interacts with side walls of the CNTs and a coating of conducting polymer on CNTs has been formed. During the last two decades, a significant number of investigations

have been made to explore the properties of polypyrrole-MWCNT composites [24-35]. But most of them have given stress on different types of preparation technique and characterization of the composites. But very few of them describe the systematic study of temperature variation of electrical conductivity and also the magnetic field dependence of electrical conductivity [36-42]. Sahoo et al [39] studied the room temperature conductivity of the PPy–MWCNT composites and concluded that the conductivity of the composites was increased by one order of magnitude than pure polypyrrole. Yu et al [40] found almost the same result. They obtained the room temperature conductivity of the composites as 0.02 S cm^{-1} whereas for pure PPy, the conductivity was 6.9 X 10^{-4} S cm^{-1}. Long et al [42] reported an improved electrical conductivity with increasing nanotube weight percentage.

In the present work, the fabrication and characterization of polypyrrole-MWCNT composites has been done. The nature of variation of electrical conductivity in the temperature range 77-300K and magnetic field dependent conductivity up to a transverse magnetic field of 1Tesla of the composites are investigated in an extensive manner.

2. Sample preparation and experimental techniques

Pyrrole monomer, Cetyltrimethylammonium bromide (CTAB), MWCNT (Nanocyl 7001), ammonium peroxydisulphate (APS), ethanol and acetone have been used as received from the market and purified. Double distilled water and pyrrole were used in this study.

Composites of polypyrrole with multiwall carbon nanotubes (MWCNT) were synthesized by in situ chemical oxidative polymerization method. CTAB have been used as a cationic surfactant. 1.136 gm CTAB and 60 mg MWCNT were added in 300 ml 1(M) HCl and the mixture was subjected to sonication to obtain a well-dispersed suspension which was then kept at 0-5^{o}C in the refrigerator. A precooled 1.2 ml pyrrole monomer and 125 ml 1(M) HCl containing 2.7 gm APS were added sequentially to the MWCNT-CTAB suspension taken in an ice chamber. During this mixing of the solutions, continuous magnetic stirring for 1 hr was done and then left standing in the refrigerator at 0-5^{o}C for 24 hr. A black precipitate was obtained on filtration. The solid mass was washed with ethanol and acetone repeatedly to remove oligomers and unreacted monomer. Then the precipitate was washed with double distilled water several times and dried at room temperature in a dynamic vacuum for 24 hr. For comparison purposes, four different samples have been prepared with 0, 1, 2 and 3 %

MWCNT. Samples were numbered as S0, S1, S2 and S3 for 0, 1, 2 and 3 % MWCNT respectively. Morphology of samples was obtained by using a Field emission scanning electron microscope. The other characterization and experimental techniques were given in our previous study [43].

3. Results and Discussion:

Fig.1 shows the XRD pattern of polypyrrole (S0) and it's composite with MWCNT (S1, S2 and S3). This XRD pattern shows a broad peak at $2\theta = 25^0$ in polypyrrole and it may arise due to regular repetition of monomer unit. In case of the composite, three peaks at 2θ = 25, 43, 50^0 are obtained. XRD pattern of MWCNT is published elsewhere [43] and it has some peaks at 2θ = 25, 43, 50^0. So the observed peaks in the composite are obtained due to the presence of MWCNT. The peak at $2\theta = 25^0$ is more broad in the composite of polypyrrole with MWCNT than pure polypyrrole, because the peak of MWCNT at $2\theta = 25^0$ has been merged with the peak of polypyrrole.

Fig. 2 represents the FESEM micrograph of MWCNT coated with polypyrrole (S2 and S3). Both rod and particle like morphologies of the composite are seen from the micrograph. Wire like morphology is obtained for the pure MWCNT which is used for our investigation and its micrograph is reported elsewhere [44]. Diameter of the composite has been increased after polymerization and it suggests that the pyrrole is uniformly spread on the surface of the MWCNT. Diameter of the rod is 50-60 nm and length is in the range 0.5-1μm. Decrease in chain entanglement and over crowding of polymer may form particle morphology.

FTIR spectrums of polypyrrole (S0) and its composite (S1) are presented in Fig. 3. Polypyrrole has characteristic peaks at 3420, 2926, 1463, 1265, 1100, 785 cm^{-1} . The band at 3420 cm^{-1} is attributed to hydrogen bonded N-H stretching vibration [45]. A small band is obtained at 2926 cm^{-1} for the C-H stretching vibration of the five membered ring of pyrrole [46]. The band at 1463 and 1265 cm^{-1} may be attributed to C-N stretching modes of vibration in pyrrole ring. The band at 782 cm^{-1} may be attributed to out of plane C-H vibration. The peak assignment reveals that the synthesized product is polypyrrole [45]. Incorporation of MWCNT in polypyrrole results in shifting of the peaks from 3420, 1463, 1100, 785 cm^{-1} to 3394,1499,1055 and 727 cm^{-1}. It indicates the interaction of MWCNT with different reaction

sites of polypyrrole. Shifting of the band at 1463 cm^{-1} indicates that MWCNT may have interaction with nitrogen site of polypyrrole in composite. It is observed from FTIR spectrum analysis, peaks at 3420, 1100, 785 cm^{-1} shifted to lower wave number and peak at 1463 cm^{-1} shifted to higher wave numbers i.e., the uniform blue or red shift is not obtained in the composite. This may be due to the change in bond strength in presence of MWCNT. This FTIR result suggests that N-H, C-H, C-C bond becomes weaker and C-N bond becomes stronger in the composite [47].

TGA of polypyrrole (S0) and its composite with MWCNT (S1 S2 and S3) have been done in the temperature range 25^0C to 700^0C and the thermograms are presented in Fig.4. Thermogram of polypyrrole shows that the mass loss began around 30^0C and about 10% weight loss occur at 100^0C. This weight loss is due to the loss of water molecules from the sample. A very small weight loss is obtained for the loss of oligomers molecules till 190^0C and then weight loss occurs gradually due to the degradation of the polymer chain. 52% weight loss occurs at 750^0C for polypyrrole. It is observed from the spectrum that composites are thermally equally stable to the polypyrrole. Thermal stability of composite increases slightly with increasing MWCNT. Since the doping percentage of MWCNT in polypyrrole is very small remarkable thermal stability is not observed in our samples.

To develop the idea about the temperature dependence of dc conductivity of the PPy-MWCNT composites, the temperature variation of dc resistivity of the samples have been measured within a range $77 \leq T \leq 300$K. The values of room temperature conductivity of different samples have been indicated in the Table I. Conductivity increases with incorporation of highly conducting MWCNT in the PPy matrix. PPy is considered as a good electron donor whereas MWCNTs are relatively good electron acceptors. So there is some interaction between the quinoid rings of PPy and MWCNTs which facilitates the charge transfer process between the two components. The localization length in MWCNT is around 10 nm [48] due to the presence of a large π-conjugated structure and hence has a high conductivity. But in case of PPy, the localization length found is only 1.55 nm resulting in a relatively poor conductivity. This value is consistent with the values (1-2 nm) reported by other investigators [49]. Thus, the strong coupling between the MWCNTs and the polymer chains enhances the average localization length and hence conductivity increases for the composite samples. Fig.5 shows the variation of dc resistivity as a function of temperature.

All the investigated samples behave like disordered semiconductors. The increase in the charge transfer process between PPy and MWCNT with increasing temperature enhances the conductivity of the samples. Generally, the temperature dependence of resistivity of a disordered semiconducting system is explained in terms of Mott's variable range hopping (VRH) model [50]. According to this model, the resistivity can be expressed as

$$\rho(T) = \rho_0 \exp\left(\frac{T_{Mott}}{T}\right)^{\gamma} \qquad (1)$$

where the VRH exponent γ determines the dimensionality of the conducting medium by the relation $\gamma = 1/(1+d)$. For three, two and one dimensional system, the possible values of γ are ¼, 1/3 and ½ respectively. ρ_o is the resistivity at infinite temperature; T_{Mott} is the Mott characteristic temperature depending on the electronic structure, and the energy distribution of the localized states and can be written as

$$T_{Mott} = \frac{16}{k_B N(E_F) L_{loc}^3} \qquad (2)$$

where k_B is the Boltzmann constant, $N(E_F)$ is the density of states at the Fermi level and L_{loc} is the localization length. To investigate the true charge transfer mechanism, the temperature dependence of dc resistivity of all the investigated samples has been analyzed by Eq.(1). A graph (Fig.5) has been plotted between ln[ρ(T)] with T for all samples. The points are the experimental data and solid lines are the theoretical values obtained from Eq.(1). The best fitted values of the parameters ρ_o, T_{Mott} and γ are listed in Table I. From the Table I, it can be shown that the value of γ for different samples is around 0.25, which suggest that three dimensional (3D) charge transport mechanism is suitable for explaining the temperature dependence of dc resistivity of the investigated samples. For the non-isolated conducting polymer chains, an extension of electronic wave functions in three dimensions happens due to the presence of conducting islands in between the insulating polymer matrix. SEM micrographs of the composite samples reveal the existence of non-isolated polymer chains and the PPy matrix encapsulates MWCNTs. The experimental data fits reasonably well with 3D VRH model. Therefore, the charge transport mechanism of the present samples can be explained well in terms of 3D VRH model that is supported by the experimental data. The

deviation from the 3D VRH model in the lower temperature range for S0 may be due to the presence of the defect states in the sample. It is also observed that values of T_{Mott} reduces by two order of magnitude after incorporating highly conducting MWCNT in PPy matrix, but its value increases with increasing MWCNT contents. This anomalous behavior of T_{Mott} may be due to the different homogeneity present in the samples. In order to clear this anomaly we have calculated the resistivity ratio ρ_r [= ρ(77K)/ρ(300K)], which is the measured of disorder. It is observed that its value is high (156.5) for S0 and reduces to 13 for S1 and again increases to 95.5 for S2 and 103.2 for S3. This suggests that disorderness of the samples has been reduced for incorporation of low concentration of MWCNT than large concentration due to inhomogenity. Due to this an anomalous change in localization length has been observed, which may be the probable reason behind the anomalous behavior of T_{Mott}, because $T_{Mott} \propto 1/ L_{loc}^{3}$.

To investigate the magnetotransport property of the PPy-MWCNT composites, the magnetic field dependent resistivities of different samples have been measured within a temperature range 77-300K and under a transverse magnetic field upto 1 Tesla. Fig.6 shows the variation of magnetoconductivity with magnetic field strength at T=300K for different samples. Conductivity of all the samples decreases with increasing magnetic field strength i.e. negative magnetoconductivity is observed in all of them. The maximum percentage changes of conductivity $\left[\frac{\sigma(B,T)-\sigma(0,T)}{\sigma(0,T)}\times 100\right]$ under a magnetic field of 0.8 Tesla at 300K are -0.07% for S0, -0.36% for S1, -0.70% for S2 and -0.86% for S3 respectively. The percentage change of magnetoconductivity is almost same as that of pure PPy but it increase with increasing content of MWCNT in the PPy matrix. In general, the dc magnetoconductivity can be analyzed by simple phenomenological model that consists of two simultaneously acting hopping processes- the wave function shrinkage model [51-52] and the forward interference model [53-55]. In wave function shrinkage model, the average hopping length reduces due to the contraction of wave function of electrons under the influence of a magnetic field. As a result, the conductivity decreases with increasing magnetic field. Under a small magnetic field, the magnetoconductivity ratio can be expressed as [51]

$$\ln\left[\frac{\sigma(B,T)}{\sigma(0,T)}\right] = -t_1 \frac{e^2 L_{loc}^4}{\hbar^2}\left(\frac{T_{Mott}}{T}\right)^{3/4} B^2 \qquad (3)$$

where t_1= 5/2016 and L_{loc} is the localization length. Again in forward interference model, direct and indirect hopping mechanisms between localized states are considered, and the phase factor that is considered by the field flux through the area between the hopping routes is averaged to show that field reduces the resistance, resulting in positive magnetoconductivity. According to this model, the magnetoconductivity ratio becomes

$$\frac{\sigma(B,T)}{\sigma(0,T)} = 1 + \frac{\frac{C_{sat}B}{B_{sat}}}{1+\frac{B}{B_{sat}}} \qquad (4)$$

where C_{sat} is a temperature independent parameter and $B_{sat} = 0.7\left(\frac{h}{e}\right)\left(\frac{8}{3}\right)^{\frac{3}{2}}\left(\frac{1}{L_{loc}}\right)^2\left(\frac{T}{T_{Mott}}\right)^{\frac{3}{8}}$. As small localization length of PPy is obtained, the average hopping length $R_{hop} = \left(\frac{3}{8}\right)\left(\frac{T}{T_{Mott}}\right)^{\frac{1}{4}} L_{loc}$ becomes smaller (indicated in the Table I) and thus, wave function shrinkage effect may be observed in PPy. However, a positive magnetoconductivity for CNT films and pellets at weak magnetic field due to their large L_{loc} and R_{hopp} has been reported in the literature [56-57]. Therefore, the competition of these two (wave function shrinkage and forward interference) effects is responsible for change in the sign and magnitude of magnetoconductivity of the PPy-MWCNT composites. In addition, we note that the magnitude of the positive magnetoconductance is much smaller than that of the negative magnetoconductance, which may reflect that the quantum interference effect is much weaker than the wave function shrinkage effect of the samples whose localization length is comparatively small [58]. Therefore, the predominance of wave function shrinkage effect over forward interference effect is indicated by the observed decrement of magnetoconductivity of the investigated samples. So the measured data has been analyzed according to the wave function shrinkage model. Fig. 6 shows the linear variation of $\ln[\sigma(B,T)/\sigma(0,T)]$ with B^2 for different samples at room temperature. The points in the graph

represent the experimental data and the curves represent the theoretical best fits according to the wave function shrinkage model. It is evident from Fig.6 that the experimental data are fitted reasonably well with the presumed theoretical model. Localization lengths have been calculated from the slopes of the graphs of Fig.6 by using Eq.(3) and are indicated in the Table I. The localization lengths of the composite samples are larger compare to S0. Due to which a greater conductivity is found in composite samples than PPy.

Fig.7 shows the variation of magnetoconductivity of S3 at different but constant temperatures. The figure shows a change of sign in magnetoconductivity from positive to negative upon increasing the temperature. The positive magnetoconductivity provides a strong evidence to support the enhancement of the average localization length of the composite at low temperature. The magnitude of the magnetoconductivity decreases with increasing temperature and ultimately negative at a temperature T = 300K due to the decrease of localization length and average hopping length. In Fig.7, the points are the experimental data while the solid lines represent the best fits obtained from Eq.(4) for temperature T = 100K, 200K, 250K and from Eq.(3) for T = 300K. It is evident from the Fig.7 that the experimental data can be well described by above theories. The localization length has been extracted from this fit and the average hopping length has also been calculated from the known values of L_{loc} and T_{Mott}. The variation of localization length of S3 is indicated in the inset of Fig.7. The average hopping length decreases from 0.33 to 0.27 nm with increasing temperature from 100 to 300K respectively and the localization length varies from 13.63nm to 8.63nm for the same temperature variation, which is consistent with the above analysis. Therefore, this anomalous behavior clearly indicates a transformation from forward interference effect (low temperature) to the wave function shrinkage effect (room temperature) in S3.

4. Conclusions

Polypyrrole MWCNT composites have been prepared by an in situ chemical oxidative polymerization method and their structural, morphological, thermal stability and conductivity studies have been carried out. The FTIR spectrum revealed that the produced product is PPy and the incorporation of MWCNT in the polymer matrix was confirmed by FTIR, XRD and FESEM studies. The electrical conductivity of the investigated samples has

been measured with and without the perpendicular magnetic field. The introduction of the highly conducting MWCNT in polymer matrix significantly increases the room temperature conductivity σ(300K) of the composite samples. The dc resistivity follows variable range hopping model. The small average hopping lengths at room temperatures give rise to a negative magnetoconductivity in PPy and PPy MWCNT composites which have been analyzed by the wave function shrinkage effect. The average hopping length decreases from 0.33 nm to 0.27 nm with increasing temperature from 100 to 300K, due to which the sign and magnitude of the magnetoconductivity changes from positive to negative, which may be due to the dominance of wave function shrinkage effect over quantum interference effect.

Acknowledgements

The authors gratefully acknowledge the principal assistance received from the MHRD, Government of India during this work.

References

[1] J. C. Aphesteguy, P. G. Bercoff, S. E. Jacobo, Phys B 398 (2007) 200.

[2] P. N. Bartlett, P. R. Birkin, Synth Met 61(1993)15.

[3] H.Naarman, Science and Application of Conducting Polymers, Adam Hilger: Bristol, England, 1991.

[4] J. Joo, A. J. Epstein, Appl Phys Lett 65 (1994) 2278.

[5] P. N. Bartlett, P. R.Birkin, Synth Met 61(1993) 15.

[6] J. A.Osaheni, A. S. Jenekhe, H.,Vanherzeele, J. S. Meth, Y. Sun, A. G. MacDiarmid, J Phys Chem 96(1992) 2830.

[7] T. Kobayashi, H. Yoneyama, H. Tamura, J Electroanal Chem161(1984) 419.

[8] Z. Hau, J. Shi, L.Zhang, M. Ruan, J.Yan, Adv Mater 14(2002) 830.

[9] B. G. Levi, Phys Today 53 (2000)19.

[10] N. Asim, S.Radiman, M. A. Bin Yarmo, Mater Lett 62 (2008) 1044.

[11] M.Omastova, M .Trchova, J .Kovarova, J.Stejskal Synth Met. 138 (2003) 447.

[12] S.P. Armes, Synth Met. 15 (1987) 61.

[13] R. Gangopadhyay, A.De, Chem. Mater. 12 (2000) 260

[14] J.H.Coller, J.P.Camp, T.W.Hudson, C.E. Schimdt, J.Biomed. Mater. Res. 50(2000) 574.

[15] Y.Sonoda, W.Takashima, K.Kaneto, Synth. Met. 121 (2001)267.

[16] N.G.Sahoo, Y.C.Jung, N.S.Goo, J.W.Cho, Macromol. Mater. Eng. 290 (2005) 1049.

[17] Q.Xiao, X.Zhou, Electrochim. Acta. 48 (2003) 575.

[18] J.Tabony, D.Tob, Nature 346 (1990) 448.

[19] P. M. Ajayan, O.Z. Zhou, Top. Appl. Phys. 80 (2001) 391.

[20] M.M. Treacy, T.W. Ebbesen, T.M.Gibson, Nature 381 (1996) 678.

[21] D.T. Colbert, Plastics Additive Compd. 18 (2003) 25.

[22] R.H. Baughman, A. A. Zakhidov, W. A. de Heer, Science 297 (2002) 787.

[23] L. Dai, A.W.H. Mau, Adv. Mater 13 (2001) 899.

[24] H. Guo, H. Zhu, H. Lin, J. Zhang, Colloid Polym. Sci. 286 (2008) 587.

[25] R. Czerw, P.M. Ajayan, Y. Sun, D.L. Carroll, Nano Lett. 1(2001) 423.

[26] J.N. Coleman, A.B. Dalton, S. Curran, A. Rubio, A. P. Davey, A. Drury, B. McCarthy, Adv Mater 12 (2000) 213.

[27] K.H. An, S. Y. Jeong, H.R. Hwang, Y. H. Lee, Adv. Mater. 16 (2004) 1005.

[28] R. J. Chen, Y.Zhang, D.Wang, H.Dai,J Am Chem Soc 123 (2001) 3838.

[29] H.T.Ham,Y.S.Choi, N. Jeong, U.Chung, Polymer 46 (2005) 6308.

[30] J.Fan, M.Wan, D.Zhu, B.Chang, Z.Pan, S.xie, J Appl. Poly. Sci. 74 (1999) 2605.

[31] K.S. Jang, H. Lee, B. Moon, Synth. Met 143 (2004) 289.

[32] G. Han, J.Yuan, G.Shi, F.Wei, Thin Solid Films 474 (205) 64.

[33] J. Liu, M. Wan, J Mater Chem 11 (2001) 404.

[34] F. Yan, G.Xue, M.Zhou J Appl Polym Sci 284 (2000) 135.

[35] M.Hughes, G.Z.Chen, M.S.P. Shaffer, D.J.Fray, A.H.Windle, chem. Mater. 14 (2002) 1610.

[36] R. Gangopadhyay, A.De, Euro Polym J 35 (1999) 1985.

[37] X. Li, B.Wu, J.Huang, J.Zhang, Z.liu, H.Li , Carbon 41 (2002) 1670.

[38] J.M.Kern, J.P. Sauvage, G.Bidan, Divisia-B.Blohorn, J Polym. Sc.: Part A: Polym. Chem. 41 (2003) 3470.

[39] N.G.Sahoo, Y.C.Jung, H.H.So, J.W.Cho, Symth. Met 157 (2007) 374.

[40] Y.Yu, C. Ouyang, Y.Gao, Z.Si, W.Chen, Z.Wang, G.Xue, J Polym. Sc.: Part A: Polym. Chem. 43 (2005) 6105.

[41] H. Zengin, W. S. Zhou, J.Y.Jin, R.Czrew, D.W.Smith,L.Echegoyen, D.L.Carroll, S.H.Foulger,J. Ballato Adv Mater 14 (2002) 1480.

[42] Y.Long, Z.Chen, X.Zhang, J.Zhang, Z.Liu, J Phys. D:Appl. Phys.37 (2004)1965.

[43] G.Chakraborty, S. Ghatak, A. K. Meikap, T. Woods, R. Babu, W. J. Blau J. Polym Sci Part B: Polym Phys 48, (2010), 1767–1775.

[44] S.Ghatak, G.Chakraborty, A. K. Meikap, T. Woods, R. Babu, W. J. Blau J. Appl. Polymer Science, 119, (2011), 1016-1025.

[45] J. Li, L. Zhu, B. Shu, H. Tang, Synth. Metals 158 (2008)396

[46] J.Jang,J.H.Oh,X.L.Li,J.Mater.Chem14 (2004)2872

[47] X. Li, G. Wang, X. Li, Sur. Coat. Tech. 197 (2005) 56

[48] J. Joo, S. M. Long, J. P. Pouget, E. J. Oh, A.G. MacDiarmid, A. J. Epstein, Phys Rev B 57 (1998) 9567.

[49] E. J. Oh, K. S. Jang, J. S. Suh, H. Kim, K. H. Kim, C. H. Yo and J. Joo, Synth. Met. 84 (1997) 147

[50] N. F.Mott, E.Davis, Electronic Process in Noncrystalline Materials, Clarendon Press, Oxford, 2nd ed.,1979.

[51] B. L. Shklovskii, Sov. Phys. Semicond. 17(1983) 1311.

[52] B. L. Shklovskii, A. L. Efros, Electronic Properties of Doped Semiconductors, Springer, Berlin, 1984, p.202.

[53] V. L. Nguyen, B. Z. Spivak, B. L. Shklovskii, Sov. Phys.-JETP. 62 (1995) 1021.

[54] U. Sivan, O. Entin-Wohiman, Y. Imry, Phys. Rev. Lett. 60 (1988) 1566.

[55] R. Rosenbaum, A. Milner, S. Hannens, T. Murphy, E . Palm, B. Brandt, Physica B 294-295 (2001) 340.

[56] M. S. Fuhrer, W. Holmes, P. L. Richards, P. Delaney, S. G. Louie, A. Zettl Synth. Met. 103 (1999) 2529.

[57] Y. Yosida, I. Oguro J. Appl. Phys. 86 (1999) 999

[58] Y. Long, Z. Chen, J. Shen, Z. Zhang, L. Zhang, K. Huang, M. Wan, A. Jin, C. Gu and J. L. Duvail, Nanotechnology 17 (2006) 5903

Figure Caption

Fig.1 XRD of PPy and different PPy-MWCNT composites

Fig.2 FESEM image of the samples S2 and S3.

Fig.3 FTIR spectrum of the samples S0 and S1

Fig.4 TGA thermograms of PPy and different PPy–MWCNT composites

Fig.5 Temperature dependence of the dc conductivity of PPy and different PPy-MWCNT composites. The solid lines are fitted to Eq.(1).

Fig.6 Variation of the dc magnetoconductivity with perpendicular magnetic field of PPy and different PPy-MWCNT composites at 300K. The solid lines are fitted to Eq.(3).

Fig.7 Variation of the dc magnetoconductivity with perpendicular magnetic field of the sample S3 at different temperatures. The solid lines are fitted to Eq.(4) for T = 300K and to Eq.(4) for T = 250K, 200K and 100K. Inset shows the variation of localization length of the sample S3 at different temperatures.

TABLE I Different physical parameters of polypyrrole–MWNT composites: Concentration of the samples in weight %, Conductivity at room temperature (σ(300K)), Temperature exponent (γ), Resistivity at infinite temperature (ρ_0), Mott characteristic temperature (T_{Mott}), Percentage change in magnetoconductivity $\left[\frac{\sigma(B,T)-\sigma(0,T)}{\sigma(0,T)}\times 100\right]$, Localization length ($L_{loc}$), Hopping length ($R_{Hopp}$)

Parameters	**S0**	**S1**	**S2**	**S3**
Concentration (wt%)	0	1	2	3
σ(300K)($\Omega^{-1}m^{-1}$)	1.57 X 10^{-2}	2..84 X 10^{-1}	1.10	1.51
γ	0.241±0.0002	0.254±0.0002	0.249±0.0002	0.248±0.0002
ρ_0 ($\Omega^{-1}m^{-1}$)	5.39 X 10^{-11}	6.26 X 10^{-3}	7.51 X 10^{-6}	3.95 X 10^{-6}
T_{Mott}(K)	2.90 X 10^{8}	4.11 X 10^{5}	5.79 X 10^{6}	5.87 X 10^{6}
$\left[\frac{\sigma(B,T)-\sigma(0,T)}{\sigma(0,T)}\times 100\right]$	-0.07	-0.36	-0.70	-0.87
L_{loc}(nm)	1.54	8.00	5.85	5.72
R_{Hopp}(nm)	0.02	0.49	0.19	0.18

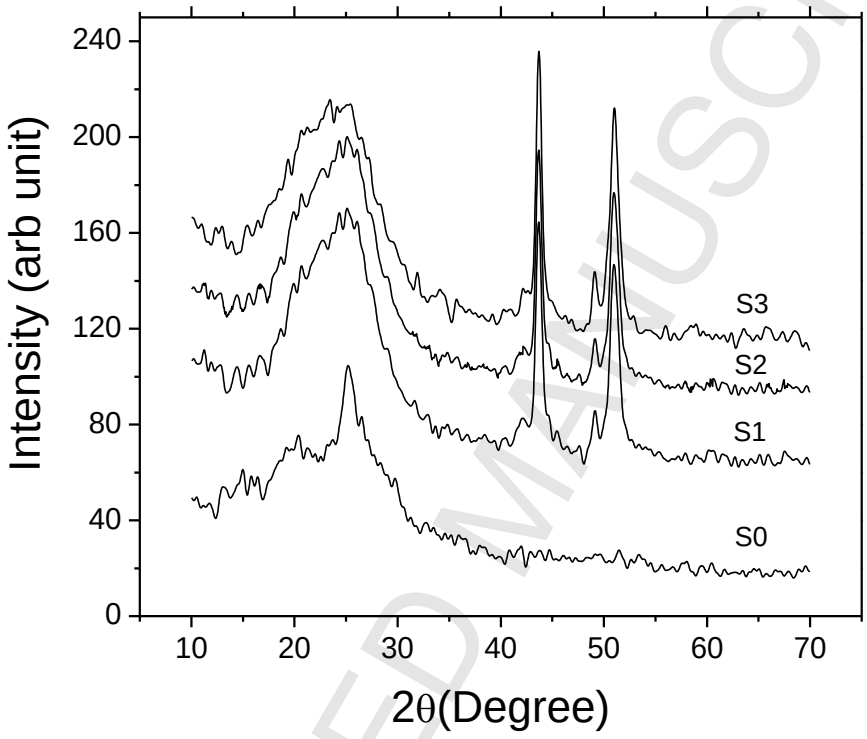

Fig.1

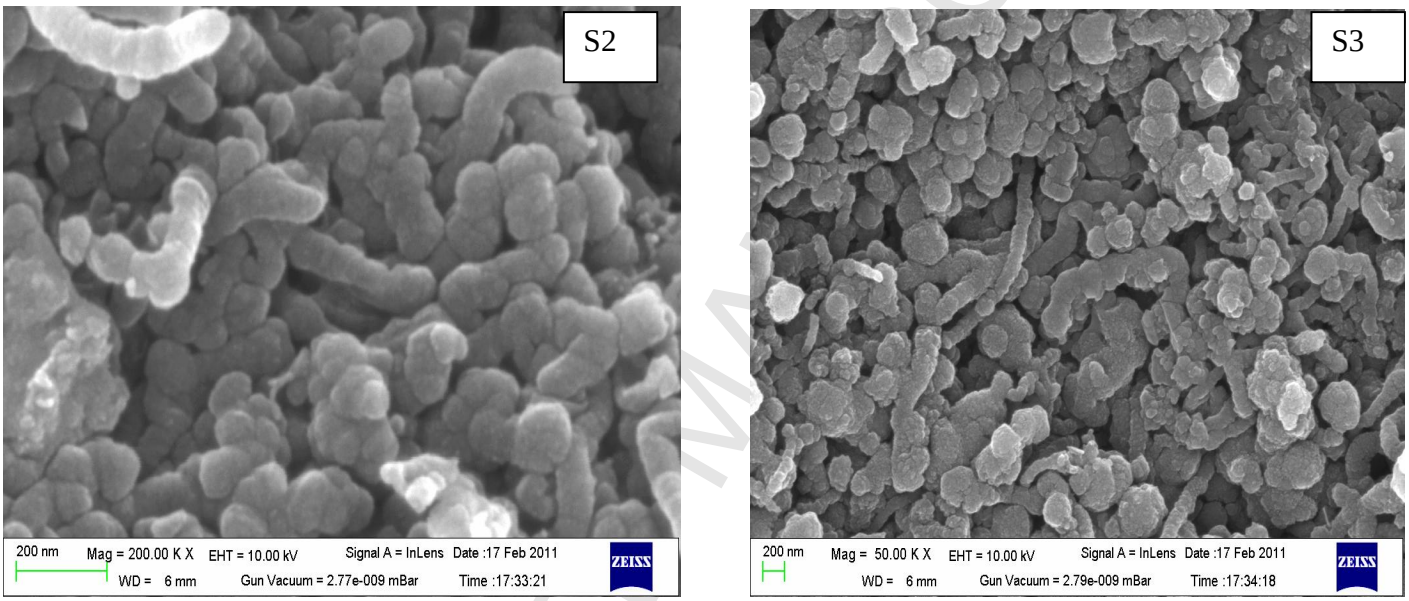

Fig.2

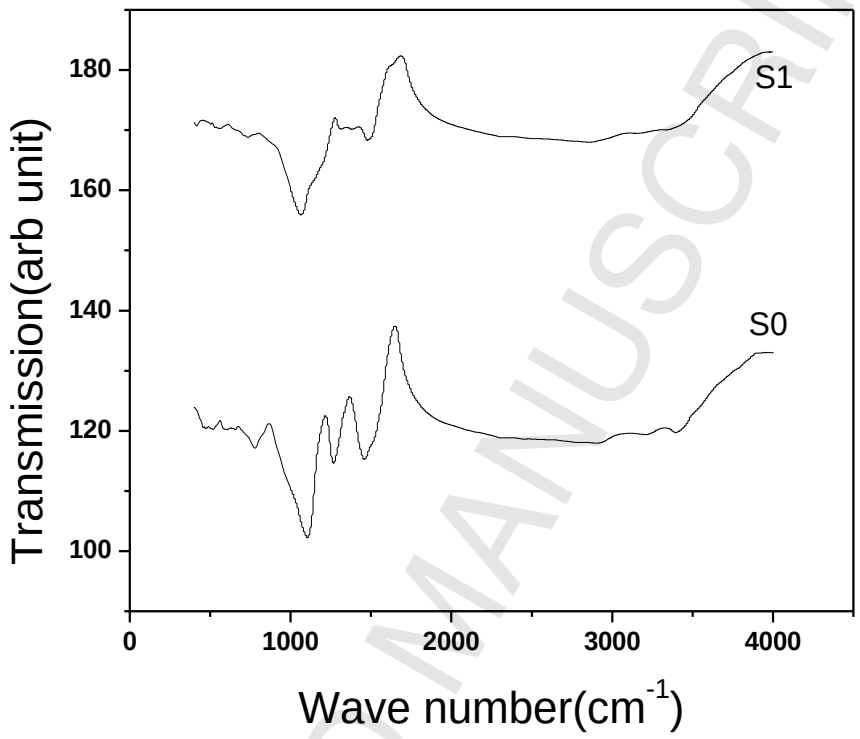

Fig.3

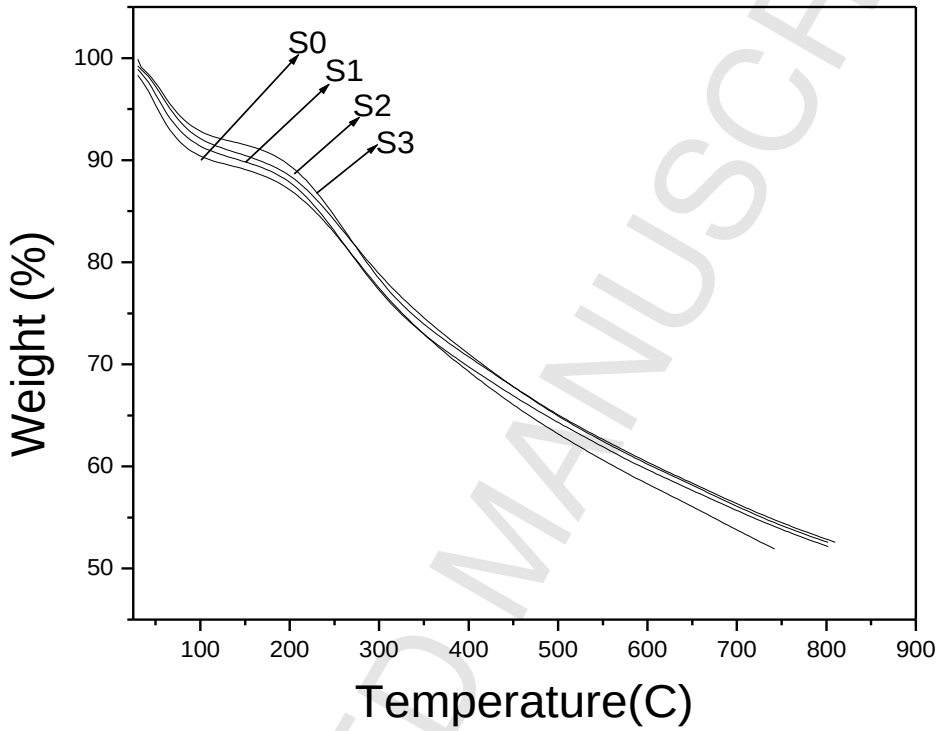

Fig.4

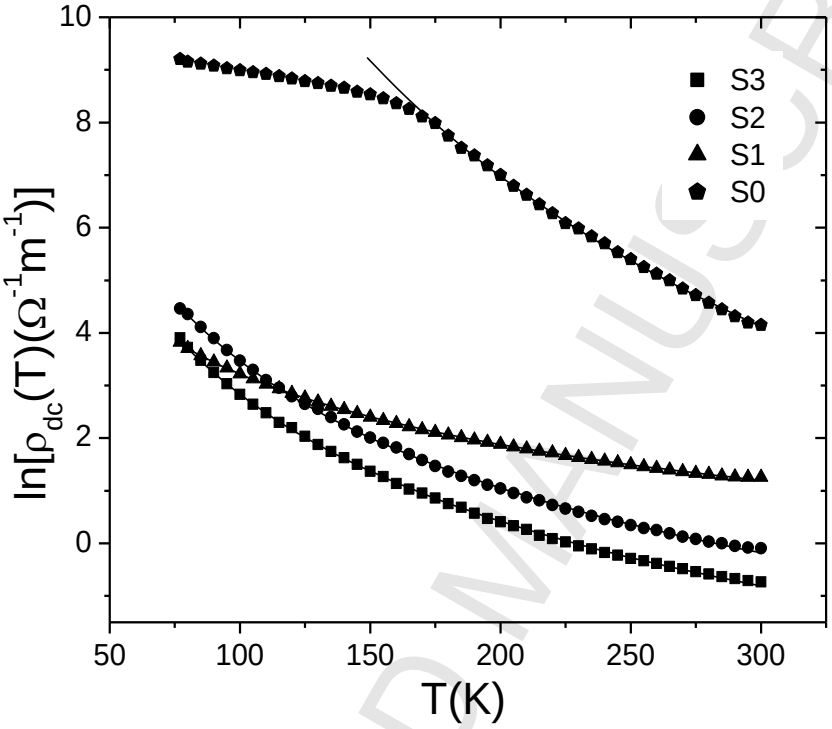

Fig.5

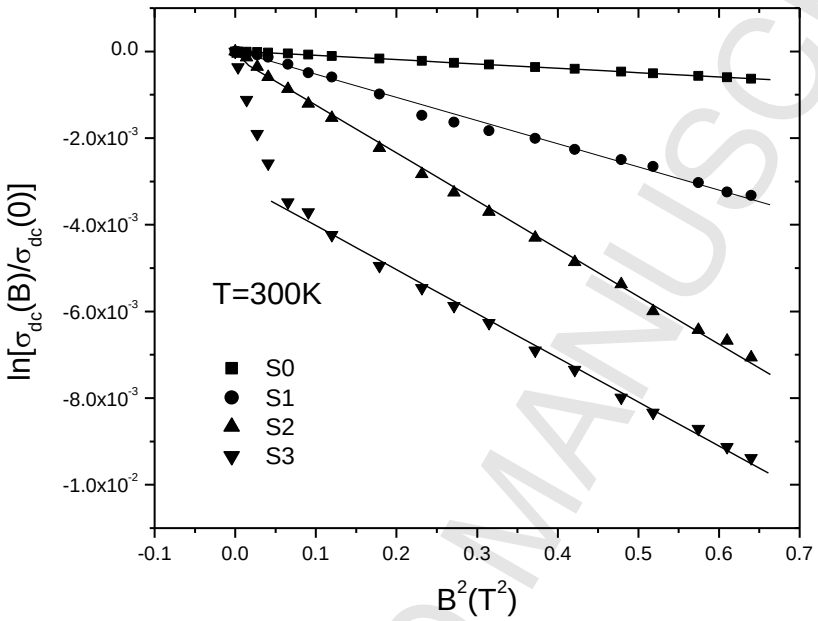

Fig.6

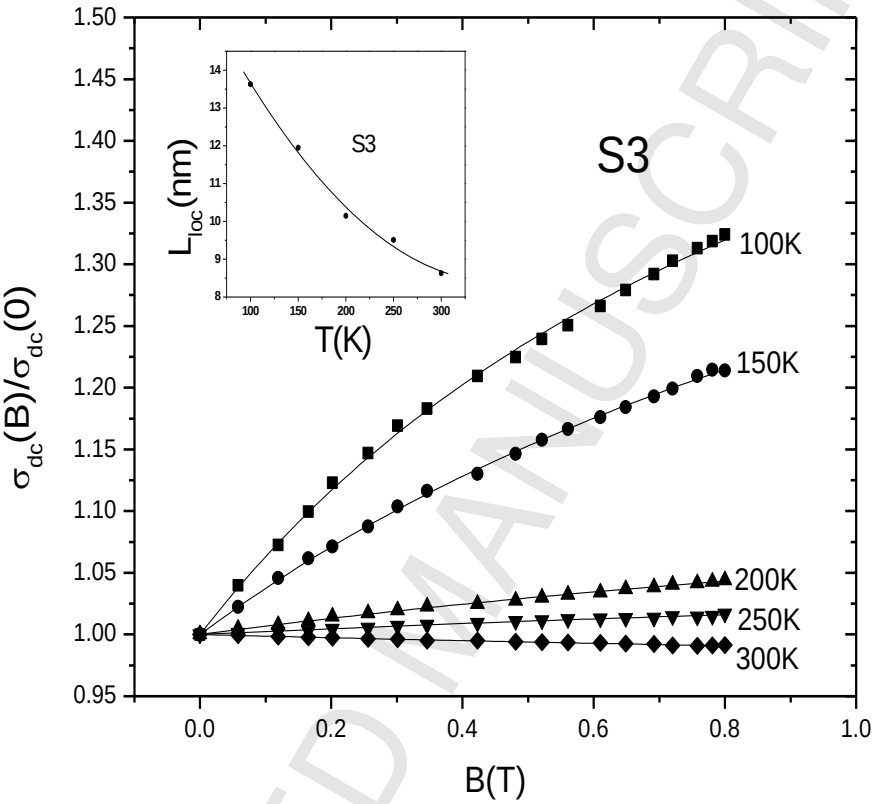

Fig.7

Highlights

> Both rod and particle like morphologies has been observe from FESEM micrograph. > FTIR spectrum analysis indicates the presence of MWCNT in polypyrrole. > Temperature variation of dc conductivity follow Mott's variable range hopping theory. > Room temperature magnetoconductivity is negative for all samples. > Observed a transformation from positive to negative magnetoconductance with increasing temperature.